International Journal of Marine Engineering Innovation and Research, Vol. 10(4), Dec. 2025. 1399-1407
(pISSN: 2541-5972, eISSN: 2548-1479)

Experimental Optimization of R-134a Refrigerant Charge in a Retrofitted Dual-Function Refrigeration System for Marine Engineering Applications

Benedicta Dian Alfanda[1*], George Endri Kusuma[2], Budhi Santoso[3], Zulfa Maulana[4], Ratna Muninggar[5]

(Received: 22 December 2025 / Revised: 4 December 2025 /Accepted: 11 December 2025 / Available Online: 20 December 2025)

***Abstract*— This paper presents an experimental optimization of R-134a refrigerant charge mass in a retrofitted dual-function vapor-compression refrigeration system designed to operate in Air-Side (AHU) and Water-Side (Water Chiller) modes. The system was evaluated after retrofit by testing four charge levels—399.5 g (85%), 423.0 g (90%), 446.5 g (95%), and 470.0 g (100%)—under multiple operating conditions: three fan speeds for AHU mode and chilled-water flowrates of 6–8 L/min for chiller mode. Performance was quantified using evaporator capacity Qevap, condenser heat rejection Qcond, compressor electrical power (PcompP_{comp}Pcomp), coefficient of performance (COP), and energy efficiency ratio (EER). The results show that the optimal charge is mode- and objective-dependent. In AHU mode, the maximum cooling capacity was obtained at 470 g (100%), reaching Qevap=4.58 kW, while the highest COPactual=3.1234 occurred at 423 g (90%), accompanied by the lowest AHU compressor power Pcomp=1.722 kW). In Water-Side mode, the highest cooling capacity was achieved at 446.5 g (95%), with Qevap=5.141 kW at 6 L/min, whereas the best energy-utilization outcome occurred at 470 g (100%) and 6 L/min, yielding EER = 2.888 with the lowest chiller compressor power Pcomp=1.6524 kW). Overall, the study provides a practical, mode-aware guideline for selecting refrigerant charge in retrofitted dual-function systems for marine engineering applications.**

***Keywords*—** Pefrigerant charge optimization, Retrofit refrigeration system, Dual-function refrigeration, Air handling unit (AHU), Water chiller, Vapor-compression cycle, Coefficient of performance (COP), Energy efficiency ratio (EER), Marine engineering applications

Corresponding Author: benedictadian@ppns.ac.id

I. INTRODUCTION

Refrigeration systems play a critical role in marine and industrial engineering applications, particularly in air conditioning, cooling processes, and thermal management systems. In marine environments, refrigeration units are commonly required to operate under varying load conditions while maintaining reliable performance and acceptable energy efficiency [1]. A two-stage system with a flash chamber, combined with appropriate refrigerant selection (e.g., R717 or R407C), can also improve cooling capacity and enhance the COP [2]. As a result, optimizing refrigeration system performance has become an important engineering challenge, especially in systems that undergo operational modifications or retrofitting [3]. A recent trend is the utilization of ship-engine waste heat to drive refrigeration systems based on absorption, ejector technology, or hybrid configurations combined with thermal energy storage. Such systems can reduce energy consumption by up to 52.4% compared with conventional electrically driven vapor-compression systems, while also lowering operating costs and emissions [4]. Many existing refrigeration systems were originally designed to operate using chlorofluorocarbon (CFC) refrigerants, such as R-12, which have been phased out due to their high ozone depletion potential. In response to international environmental regulations, hydrofluorocarbon (HFC) refrigerants such as R-134a have been widely adopted as replacement working fluids [5].

Although R-134a offers significantly lower environmental impact, direct replacement without proper system adjustment may lead to suboptimal performance, excessive operating pressure, or increased energy consumption. Therefore, retrofit processes require careful evaluation to ensure that the modified system operates safely and efficiently [6]. Several studies indicate that alternative refrigerants such as R-513A, R-450A, MC-134, and MC-22 can be used as replacements for R-134a with comparable or slightly improved

Benedicta Dian Alfanda, Departement of Marine Engineering, Shipbuilding Institute of Polytechnic Surabaya, Surabaya, 60111, Indonesia, E-mail: benedictadian@ppns.ac.id
George Endri Kusuma, Departement of Sustainable Energy Engineering Technology, Surabaya, 60111, Indonesia, E-mail: kusuma.george@ppns.ac.id
Budhi Santoso, Department of Naval Architecture, Politeknik Negeri Bengkalis, Bengkalis, 28711, E-mail: budhisantoso@polbeng.ac.id
Zulfa Maulana, Departement of Engineering, PT Dok Warisan Pertama (PAX OCEAN), Brigjen Katamso, Tanjung Uncang, Batu Aji, Batam, Indonesia, 29424, E-mail: zulfamaulana08@gmail.com
Ratna Muninggar, Departement of Marine Engineering, Shipbuilding Institute of Polytechnic Surabaya, Surabaya, 60111, Indonesia, E-mail: ratnamuninggar@ppns.ac.id

performance, provided that the system is properly configured. For example, R-513A and R-450A can be applied in R-134a-based systems with only a very small change in energy consumption (approximately −1.6% to +1.2% for R-513A) and without significant changes in condensing pressure; however, adjustments to the expansion valve are often required [7]. MC-134 and MC-22 have also demonstrated better energy efficiency and faster pull-down (temperature reduction) performance; however, their flammability characteristics must be carefully considered [8]. The effectiveness of a retrofit strongly depends on the system configuration and key components such as the compressor, evaporator, condenser, and expansion valve. Certain systems such as those using centrifugal compressors may require component modifications to maintain optimal performance when operating with a new refrigerant [9]. One of the most influential parameters in a retrofitted refrigeration system is the refrigerant charge mass. An insufficient refrigerant charge can reduce cooling capacity and system stability, while excessive charge may cause high discharge pressure, increased compressor power consumption, and potential safety risks. This issue becomes more complex in refrigeration systems that operate in multiple modes, such as dual-function systems serving both air handling units (AHU) and water chiller applications. In such systems, operating characteristics differ significantly depending on airflow rate, water flowrate, and heat load conditions, making the determination of an optimal refrigerant charge particularly challenging. Determining the optimal refrigerant charge mass is also essential for achieving the best energy efficiency [10].

Previous studies have reported that refrigerant charge optimization strongly affects system performance indicators such as cooling capacity, coefficient of performance (COP), and energy efficiency ratio (EER). However, most existing works focus on single-function refrigeration systems, such as residential air conditioners or household refrigerators [11]. Without proper adjustments, the risk of excessive operating pressure, leakage, or a reduction in COP (coefficient of performance) increases [12]. Limited experimental research addresses refrigerant charge optimization in dual-function refrigeration systems, especially those applied in laboratory-scale or marine engineering contexts where flexibility of operation is required [13]. Moreover, studies that specifically evaluate charge optimization after retrofitting from R-12 to R-134a in such systems remain scarce [14]. An experimental study conducted at the Fluid Machinery Laboratory of the Shipbuilding Polytechnic Institute of Surabaya investigated the effect of R-134a charge mass variation on a dual-function refrigeration system (air handling unit and water chiller) after retrofitting from R-12. The study found that the highest Energy Efficiency Ratio (EER), 2.888, was achieved in water chiller mode with a chilled-water flowrate of 6 L/min and a refrigerant charge of 470 g [15]. Several other studies have examined charge optimization in dual-evaporator systems or systems with operational flexibility; however, they generally employ alternative refrigerants (e.g., R290/R600a) and do not specifically address retrofitting from R-12 to R-134a or the context of marine/laboratory applications [16].

In marine engineering education and research laboratories, dual-function refrigeration systems are commonly used as experimental platforms to study vapor compression cycles under different operating modes. These systems provide valuable insight into real operational behavior but also require proper retrofit and optimization to ensure safe and energy-efficient operation. Without a systematic evaluation of refrigerant charge mass, retrofitted systems may operate outside their optimal range, limiting their effectiveness as both teaching and research facilities [17]. Another study on a dual-evaporator system using a hydrocarbon mixture found that the minimum energy consumption (1.60 kWh per 24 hours) was achieved with a 300 g refrigerant charge, a 50% mass fraction of R600a, and a 10% opening of the freezer throttle valve [18].

This study aims to experimentally optimize the R-134a refrigerant charge mass in a retrofitted dual-function refrigeration system operating as an air handling unit and a water chiller. The optimization is conducted by evaluating system performance under several refrigerant charge conditions and operating modes [19]. Key performance parameters, including evaporator capacity, condenser heat rejection, compressor power consumption, COP, and EER, are analyzed to identify the charge condition that provides balanced performance and energy efficiency [20]. The findings of this research are expected to contribute practical insights into retrofit optimization strategies for dual-function refrigeration systems, particularly for marine engineering applications and experimental facilities.

II. METHOD

A. System Description and Retrofit Background

The experimental investigation was conducted on a dual-function vapor-compression refrigeration system capable of operating in two configurations: air-side evaporator mode (Air Handling Unit, AHU) and water-side evaporator mode (Water Chiller) [21]. The system was originally designed to operate with R-12 refrigerant and was subsequently retrofitted to R-134a to comply with environmental regulations and laboratory operational requirements.

The retrofit process included removal of the original refrigerant, system evacuation, inspection of key components, leak testing, and charging with R-134a prior to experimental testing. After retrofit, the system was configured to allow controlled switching between AHU and water-chiller operation through valve adjustment and control selection.

B. Experimental Strategy and Refrigerant Charge Definition

This study adopts an experimental optimization approach by systematically varying the refrigerant charge mass and evaluating the resulting performance and energy efficiency of the system.

The reference charge (100%) was defined experimentally as the maximum refrigerant mass that allowed stable operation without abnormal high-pressure release. Based on preliminary testing, the reference charge was established at 470 g of R-134a. From this reference, four charge levels were investigated:

85%: 399.5 g
90%: 423.0 g
95%: 446.5 g
100%: 470.0 g

These charge levels were selected to capture undercharged, near-optimal, and fully charged operating conditions commonly encountered during retrofit processes.

C. Operating Modes and Test Matrix

Experiments were conducted under both functional modes of the system to reflect its dual-use characteristics: Air-side mode (AHU): tests were performed at Water-side mode (Water Chiller): tests were performed at chilled-water flowrates of 6, 7, and 8 L/min.

For each refrigerant charge level, all operating modes were tested to ensure consistent comparison of performance trends across different thermal loading conditions.

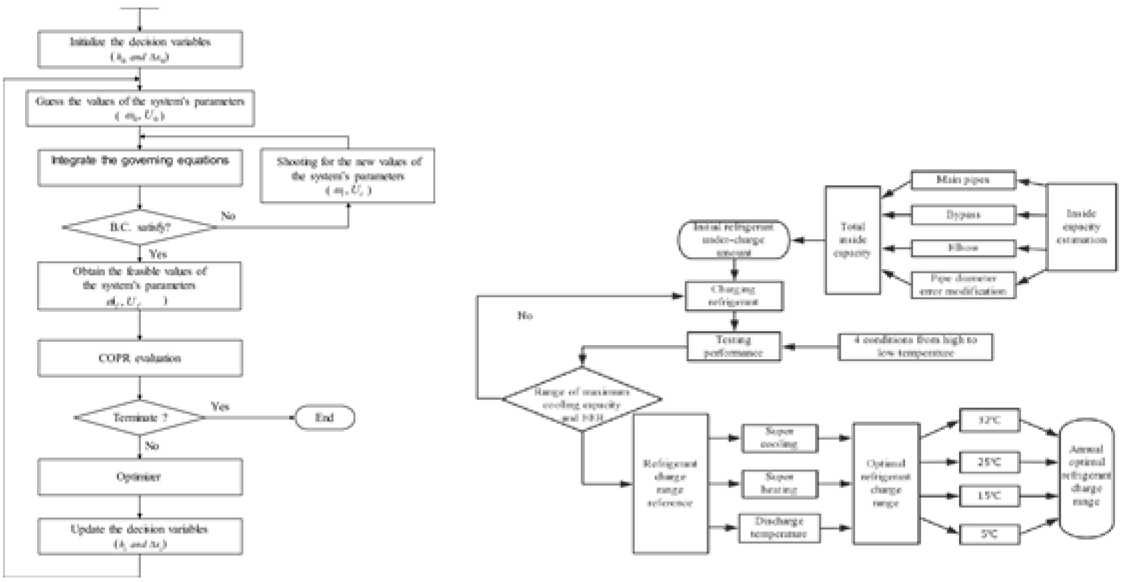

Figure. 1. Experimental Flowchart of the Study

A. Instrumentation and Measured Parameters

The refrigeration system is equipped with built-in measurement instruments commonly used in laboratory-scale refrigeration analysis. During each experimental run, the following parameters were recorded [22]:

1. Temperatures at critical points of the refrigeration cycle (compressor suction, compressor discharge, and liquid line)
2. Pressures on the low-pressure and high-pressure sides
3. Water flowrate in condenser and chiller circuits
4. Electrical parameters, including compressor input voltage and current

These measurements form the basis for thermodynamic performance calculations and energy efficiency evaluation.

B. Experimental Procedure

To ensure repeatability and reduce experimental bias, each test condition followed an identical procedure[23]:

1. The system was evacuated prior to charging to remove residual refrigerant and non-condensable gases.
2. R-134a refrigerant was charged using a calibrated refrigerant scale until the target mass was reached.
3. The system was operated until steady-state conditions were achieved, indicated by stabilized pressure and temperature readings.
4. Once stable, all required parameters were recorded for the selected operating mode.
5. The procedure was repeated for all charge levels and operating configurations.

Mode switching between AHU and water-chiller operation was performed according to the system's operational sequence to maintain consistent refrigerant and fluid flow paths.

C. Performance and Energy Efficiency Evaluation

System performance was evaluated using standard vapor-compression refrigeration relations. The following indicators were calculated [24]:

- Evaporator cooling capacity ($\dot{Q}_{evap}$)
- Condenser heat rejection ($\dot{Q}_{cond}$)
- Compressor electrical input power, determined from measured voltage and current
- Coefficient of Performance

$$\mathrm{COP} = \frac{Q_{evap}}{W_{Comp}} \tag{1}$$

Where:
$\dot{Q}$evap = Evaporator cooling capacity
$\dot{Q}$cond = Condenser heat rejection

- Energy Efficiency Ratio (EER): defined as the ratio between cooling capacity and compressor electrical input power[25].

Thermodynamic properties required for performance calculations were obtained using engineering calculation tools and cycle analysis software as supporting verification [26].

Measurement uncertainty was considered to assess the reliability of experimental results. The primary sources of uncertainty arise from temperature measurement, pressure gauges, flowmeters, and electrical measurement instruments [27].

Uncertainty propagation for calculated parameters such as cooling capacity, compressor power, COP, and EER was estimated using the root-sum-square (RSS) method, assuming independent measurement errors. Temperature and pressure uncertainties directly influence the determination of refrigerant thermodynamic properties, while voltage and current uncertainties affect the calculated compressor power.

Although minor variations are inevitable in laboratory-scale experiments, the uncertainty analysis confirms that observed performance trends among different refrigerant charge levels are significantly larger than the estimated measurement uncertainty, supporting the validity of the optimization results.

The cooling capacity of the evaporator represents the rate of heat absorbed from the conditioned medium (air or chilled water) and is expressed as:

$$Q_{evap} = m_{ref}(h1 - h4) \quad (2)$$

Where:
Q_{evap} = Evaporator cooling capacity (kW)
$\dot{m}_{ref}$ = Refrigerant mass flow rate (kg/s)
h1 = Refrigerant specific enthalpy at evaporator outlet / compressor inlet (kJ/kg)
h4 = Refrigerant specific enthalpy at evaporator inlet (kJ/kg)

Condenser Heat Rejection The heat rejected by the condenser is calculated as[28]:

$$Q_{cond} = m_{ref}(h2 - h3) \quad (3)$$

Where:
$\dot{Q}$cond =Condenser heat rejection rate (kW)
h2 = Refrigerant specific enthalpy at compressor Outlet(kJ/kg)
h3 = refrigerant specific enthalpy at condenser outlet (kJ/kg)

Compressor Power Consumption, The electrical power input to the compressor motor was determined from measured electrical parameters using [29]:

$$P_{comp} = \sqrt{3}\, V\, I \cos\emptyset \quad (4)$$

Where:
Pcomp = compressor electrical input power (kW)
V = line voltage (V)
I = line current (A)
cosϕ = power factor (–)

Coefficient of Performance (COP), The refrigeration system performance is expressed using the coefficient of performance (COP), defined as [30]:

$$COP = \frac{Q_{evap}}{P_{comp}} \quad (5)$$

The COP provides a direct indication of how effectively the input electrical power is converted into useful cooling output [31].

To assess compressor loading under different refrigerant charges, the pressure ratio is defined as [32]:

$$PR = \frac{P_{dis}}{P_{suc}}$$

Where:
Pdis =Compressor discharge pressure
Psuc = Compressor suction pressure

The pressure ratio provides insight into compressor stress and operational stability following refrigerant charge variation.

TABLE 1.
AIR SIDE (AHU) PERFORMANCE SUMMARY FOR EACH CHARGE AND FAN SPEED

Charge (g, %)	Fan speed	Q_evap (kW)	Q_cond (kW)	COP_ideal	COP_actual	P_comp (kW)	EER
399.5 (85%)	1	4.556	6.176	5.093	2.812	1.8305	2.4887
399.5 (85%)	2	4.496	6.109	5.0482	2.7872	1.835	2.4501
399.5 (85%)	3	4.556	6.176	5.093	2.812	1.841	2.4745
423 (90%)	1	3.812	5.044	5.2861	3.0936	1.7504	2.1776
423 (90%)	2	3.812	5.047	5.3231	3.0861	1.722	2.2136
423 (90%)	3	3.868	5.106	5.2536	3.1234	1.7461	2.2151
446.5 (95%)	1	3.163	4.208	5.2015	3.0265	1.7768	1.7802
446.5 (95%)	2	3.163	4.206	5.1657	3.0337	1.7813	1.7757
446.5 (95%)	3	3.163	4.203	5.1305	3.0409	1.7827	1.7744
470 (100%)	1	4.527	6.08	4.9006	2.9144	1.7242	2.6253
470 (100%)	2	4.525	6.114	5.0537	2.846	1.7447	2.5934
470 (100%)	3	4.58	6.156	5.2088	2.9067	1.7534	2.6123

III. RESULTS AND DISCUSSION

1. Overall performance trends across refrigerant charge

The retrofitted dual-function system was evaluated in two operating modes: Air Side (AHU) with three fan speeds and Water Side (water chiller) with three chilled-water flowrates. Across both modes, changing the R-134a charge (399.5–470 g) clearly shifted (i) cooling capacity at the evaporator, (ii) heat rejection at the condenser, and (iii) efficiency indicators (COP and EER). The results show that the “best” charge depends on the optimization objective: maximum cooling capacity, maximum COP, or maximum EER / minimum compressor power, especially for the water-chiller duty where marine applications typically demand stable heat extraction.

2. Air Side (AHU) performance under refrigerant-charge variation

Table 1 summarizes the air-side (AHU) performance of the retrofitted dual-function refrigeration system under four R-134a charge levels (85%, 90%, 95%, and 100%) and three fan-speed settings. Overall, the results indicate that refrigerant charge has a stronger influence on system behavior than fan speed within the tested range. In terms of cooling capacity, the highest evaporator capacity was obtained at the full charge condition, reaching 4.58 kW at 470 g (100%) with Fan Speed 3, which suggests that a fully charged system provides the greatest cooling output for AHU operation. From an efficiency standpoint, the best actual COP was achieved at a moderate charge level, with COP_actual = 3.1234 at 423 g (90%) and Fan Speed 3, indicating that a slightly reduced charge can enhance thermodynamic efficiency in air-side mode. Consistently, the lowest compressor electrical power was also observed near this charge level, with a minimum of 1.722 kW at 423 g (90%) and Fan Speed 2, reflecting reduced compressor loading. In contrast, when efficiency is expressed using EER, the highest value occurs at the full charge condition, reaching EER = 2.6253 at 470 g (100%) and Fan Speed 1, and remaining relatively high across fan speeds. Across the three fan-speed settings, the variations in Q_{evap}, COP_{actual}, and compressor power are comparatively small at a fixed charge level, reinforcing that charge optimization is the primary lever for improving AHU performance. These findings imply a trade-off for air-side operation: 470 g (100%) is preferable when maximum cooling capacity is prioritized, whereas 423 g (90%) is more favorable when the objective is to maximize actual COP and reduce compressor power demand.

3. Water Side (water chiller) performance under refrigerant-charge variation

For marine engineering applications, the water-chiller mode is often the critical duty because it can be integrated with cooling loops and auxiliary loads. Table 4 reports the comparative results for each charge at 6, 7, and 8 L/min.

TABLE 2.
WATER SIDE (WATER CHILLER) PERFORMANCE SUMMARY FOR EACH CHARGE AND FLOWRATE

Charge (g, %)	Flowrate (L/min)	Q_evap (kW)	Q_cond (kW)	COP_ideal	COP_actual	P_comp (kW)	EER
399.5 (85%)	6	4.772	6.312	5.03	3.0987	1.7753	2.688
399.5 (85%)	7	4.778	6.257	4.9038	3.2303	1.7725	2.695
399.5 (85%)	8	4.829	6.138	5.0721	3.6866	1.7329	2.786
423 (90%)	6	4.713	6.084	5.5702	3.4367	1.7957	2.624
423 (90%)	7	4.656	6.049	5.4823	3.3438	1.8132	2.568
423 (90%)	8	4.656	6.046	5.4427	3.3519	1.8236	2.553
446.5 (95%)	6	5.141	6.577	5.6075	3.5806	1.8341	2.803
446.5 (95%)	7	5.071	6.534	5.6295	3.4667	1.8399	2.756
446.5 (95%)	8	5.065	6.534	5.7833	3.4468	1.875	2.701
470 (100%)	6	4.772	6.335	4.9593	3.053	1.6524	2.888
470 (100%)	7	4.766	6.335	5.1186	3.0385	1.6683	2.857
470 (100%)	8	4.71	6.273	5.0755	3.013	1.67	2.82

Table 2 presents the water-side (water chiller) performance of the retrofitted refrigeration system for four R-134a charge levels (85–100%) under three chilled-water flowrates (6–8 L/min). The results indicate that the optimal charge depends on whether the priority is cooling capacity, COP, or energy-efficiency ratio. In terms of cooling output, the highest evaporator capacity was achieved at the 95% charge condition, reaching Qevap=5.141Q_{evap}=5.141Qevap=5.141 kW at 446.5 g (95%) and 6 L/min, and this operating point also produced the highest condenser heat rejection (Qcond=6.577Q_{cond}=6.577Qcond=6.577 kW), suggesting that a slightly reduced charge can maximize heat transfer performance in chiller operation. When efficiency is evaluated using actual COP, the best performance occurred at the lowest charge combined with the highest flowrate, where COP_{actual}=3.6866 was obtained at 399.5 g (85%) and 8 L/min, indicating that increased chilled-water flow can enhance the effective cooling-to-power ratio under a lower charge condition. However, the energy-efficiency ratio (EER) reaches its maximum at full charge, with EER = 2.888 at 470 g (100%) and 6 L/min, which coincides with the lowest compressor power in the table Pcomp=1.6524 kW. This shows that, for water-side operation, a full charge can reduce compressor electrical demand and deliver the highest EER, particularly at lower flowrates. Across the 470 g series, EER decreases slightly as flowrate increases (from 2.888 at 6 L/min to 2.820 at 8 L/min), implying that higher flowrate does not necessarily translate into better overall energy efficiency when compressor power is considered. Overall, these findings highlight a practical trade-off for chiller applications: 95% charge is preferable when maximum cooling capacity is targeted, 85% charge at higher flow favors maximum actual COP, and 100% charge is most advantageous when prioritizing EER and reduced compressor power for energy-conscious operation.

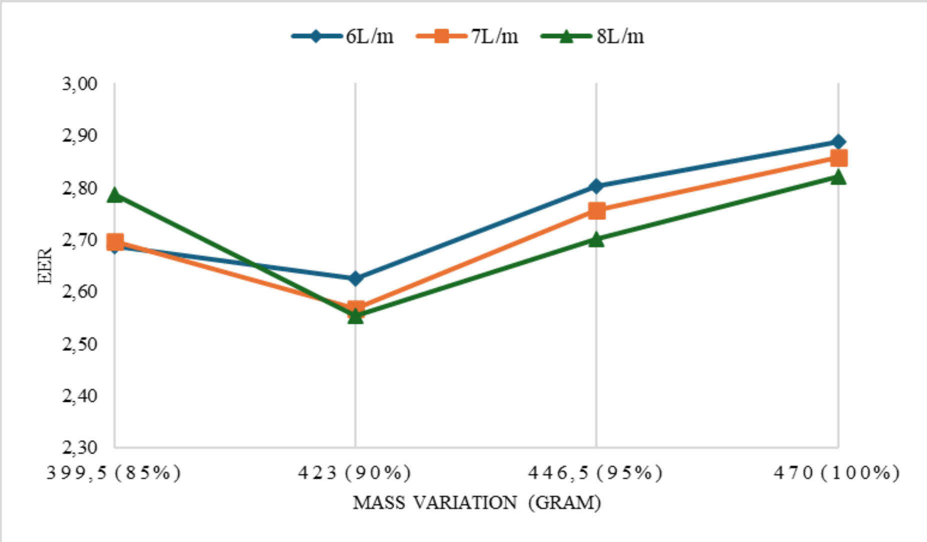

Figure. 2. Graph of the relationship between EER values and each refrigerant mass variation in Water-Side mode (Water Chiller).

The figure illustrates the relationship between EER and R-134a refrigerant charge mass in Water-Side (Water Chiller) mode at three chilled-water flowrates (6, 7, and 8 L/min). A consistent trend is observed across all flowrates: when the charge increases from 399.5 g (85%) to 423 g (90%), the EER decreases, indicating a temporary reduction in energy efficiency at the 90% charge condition. As the charge is increased further to 446.5 g (95%), the EER rises again for all flowrates, suggesting that the system operates more efficiently near this charge range. The EER then continues to improve at the full charge condition, and the highest value is achieved at 470 g (100%) with 6 L/min, where the system reaches its maximum EER. In addition, at both 95% and 100% charge, the curve for 6 L/min remains above those for 7 and 8 L/min, indicating that EER tends to decrease as the chilled-water flowrate increases. This behavior implies that higher flowrates may increase the compressor electrical demand relative to the cooling effect, thereby lowering the energy efficiency ratio. Overall, the figure confirms that, under water-side operation, a near-full to full refrigerant charge combined with a lower chilled-water flowrate provides the most favorable EER performance.

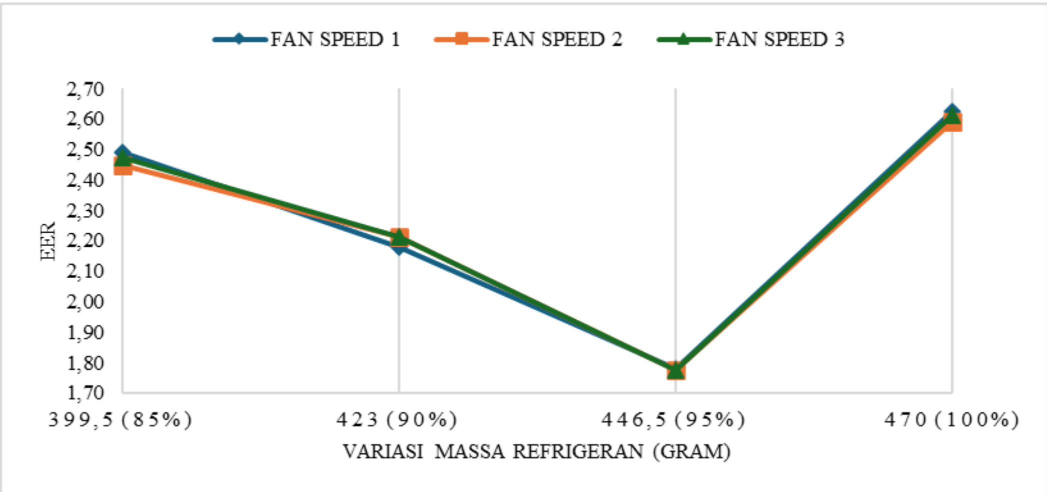

Figure. 3. Graph of the relationship between EER values and each refrigerant mass variation in Air-Side mode (AHU).

Figure 4 illustrates the relationship between EER and R-134a refrigerant charge mass in the Air-Side (AHU) mode at three fan-speed settings. The curves show a consistent trend for all fan speeds: the EER is relatively high at 399.5 g (85%), decreases at 423 g (90%), reaches its lowest level at 446.5 g (95%), and then increases sharply to its highest value at 470 g (100%). This indicates that the system experiences a noticeable reduction in energy efficiency near the 95% charge condition, while the full-charge condition provides the most favorable EER performance in AHU operation. In addition, the three fan-speed curves are closely clustered across all charge levels, suggesting that fan speed has only a minor effect on EER compared to refrigerant charge within the tested range. Overall, the figure confirms that optimizing the refrigerant charge is the primary factor for improving EER in air-side operation, with the best energy-efficiency ratio achieved at the 470 g (100%) charge level.

4. Discussion

The results confirm that refrigerant charge optimization in a retrofitted dual-function system is inherently multi-objective, because the "best" charge depends on whether the target is maximum cooling capacity, maximum COP, or maximum energy efficiency (EER) with reduced compressor burden. In air-side (AHU) operation, the full-charge condition provides the largest cooling output, with the maximum evaporator capacity reaching 4.58 kW at 470 g (100%) and Fan Speed 3. However, the most efficient operating point in terms of actual COP occurs at a slightly reduced charge: COP_actual peaks at 3.1234 for 423 g (90%) and Fan Speed 3, while compressor power is also minimized near this region (1.722 kW at 423 g and Fan Speed 2). This behavior suggests that, in AHU mode, moving away from full charge can reduce compressor loading and improve the useful cooling-to-power balance, even though it may not maximize absolute cooling capacity. Importantly, changes in fan speed cause only modest variations when the charge is fixed, indicating that charge selection is the dominant lever for improving AHU performance within the tested fan-speed range.

In water-side (water chiller) operation, the trade-off becomes clearer and more practically relevant for marine engineering duty cycles. The system delivers its highest cooling capacity at the near-full charge condition, achieving Qevap=5.141 kW at 446.5 g (95%) and 6 L/min, alongside the highest condenser heat rejection Qcond=6.577 kW. This indicates that a slightly reduced charge can enhance heat transfer effectiveness and provide capacity reserve in chiller mode. In contrast, the highest thermodynamic efficiency (actual COP) is obtained at a lower charge and higher water flowrate, where $CO_{Pactual}$=3.6866=3.6866 is achieved at 399.5 g (85%) and 8 L/min—a result that is consistent with improved heat pickup at the evaporator under higher flow conditions, although it does not maximize capacity. From an energy-utilization perspective, the strongest outcome is observed at full charge and low flowrate: EER reaches 2.888 at 470 g (100%) and 6 L/min, which coincides with the lowest compressor power in the water-side dataset Pcomp=1.6524 kW. Notably, EER at 470 g decreases slightly as flowrate increases (2.888 → 2.857 → 2.820), showing that increasing flowrate does not automatically translate into better overall energy efficiency once compressor electrical demand is considered.

From an application standpoint, these findings provide a practical selection framework for marine-engineering-related refrigeration duties. If the system is intended to prioritize cooling capacity and load-handling robustness (e.g., fast pull-down or higher thermal loads), the water-side results support ~446.5 g (95%) as a strong candidate. If the goal is to maximize actual COP under high-flow chiller operation, the best point shifts toward ~399.5 g (85%). Meanwhile, if the dominant constraint is energy efficiency and reduced compressor burden, the evidence favors ~470 g (100%), particularly at lower chilled-water flowrates. Therefore, rather than a single "universal optimum," the study supports a mode-aware, objective-driven charge recommendation—a valuable insight for systems that must operate flexibly as both an AHU and a water chiller.

5. Novelty and Contribution to the Literature

Dual-function perspective (AHU + Water Chiller): Unlike many charge-optimization studies that focus on single-function air conditioners or standalone chillers, this study maps refrigerant-charge effects in a dual-mode refrigeration system, demonstrating that optimal charge can shift depending on operating mode and load representation.

Post-retrofit charge optimization for an educational/marine engineering platform: The study addresses a practical gap in retrofit implementation by experimentally defining and testing charge levels for an R-12 to R-134a retrofitted system, providing engineering guidance for safe and efficient post-retrofit operation in laboratory-scale marine engineering facilities. Multi-objective optimization outcome capacity vs COP vs EER): The paper does not report only a single "best" condition; instead, it provides an engineering decision framework showing distinct optima for maximum capacity (95% in chiller mode), maximum COP (85% at high flow), and maximum EER with minimum compressor power (100% at low flow). This makes the results more actionable for real operational constraints.

IV. CONLUSION

This study experimentally investigated the effect of R-134a refrigerant charge mass on the performance of a retrofitted dual-function vapor-compression refrigeration system operating in Air-Side (AHU) and Water-Side (Water Chiller) modes. Four charge levels were evaluated—399.5 g (85%), 423.0 g (90%), 446.5 g (95%), and 470.0 g (100%)—to determine the charge condition that best supports system performance and energy efficiency under different operating demands. The results confirm that refrigerant charge is a dominant factor affecting cooling capacity, compressor electrical power, and efficiency indicators (COP and EER), while the influence of fan speed (air-side) and flowrate (water-side) mainly modifies the trends within a narrower range. In AHU mode, the maximum cooling capacity was achieved at the full-charge condition, with the highest evaporator capacity reaching Qevap=4.58 kW at 470 g (100%) (Fan Speed 3). However, the best efficiency based on actual COP was obtained at a moderate charge, where $CO_{Pactual}$=3.1234at 423 g (90%) (Fan Speed 3), and the lowest compressor power in the AHU dataset occurred at Pcomp=1.722 kW (423 g, Fan Speed 2). In Water-Side mode, the highest cooling capacity was obtained near full charge at 446.5 g (95%), achieving Qevap=5.141 kW at 6 L/min, while the maximum COPactual=3.6866 was observed at 399.5 g (85%) and 8 L/min. From an energy-utilization perspective, the most favorable water-side operation was found at the full-charge condition and low flowrate, where EER = 2.888 and Pcomp=1.6524 kW were achieved at 470 g (100%) and 6 L/min, indicating reduced compressor burden with improved energy efficiency.

Overall, this work demonstrates that the “optimal” refrigerant charge for a retrofitted dual-function system is objective-dependent. For practical implementation, 470 g (100%) is recommended when prioritizing higher EER and lower compressor power, 446.5 g (95%) is preferable when prioritizing maximum water-side cooling capacity, and 423 g (90%) is suitable when prioritizing higher COP in AHU operation. These findings provide a mode-aware guideline for refrigerant charge selection in retrofitted dual-function refrigeration systems intended for marine engineering applications and laboratory-scale operational flexibility.

Future work may include extending the test matrix to wider load variations and ambient conditions, evaluating long-term stability after retrofit, and conducting a more detailed uncertainty quantification for calculated performance parameters under dynamic operating behavior

ACKNOWLEDGEMENTS

The authors gratefully acknowledge the support of the Fluid Machinery Laboratory, Shipbuilding Institute of Polytechnic Surabaya, for providing experimental facilities and technical assistance during this research. The authors also thank the laboratory staff for their support in system preparation and data collection.

REFERENCES

[1] O. Yilmaz, H. Bayar, V. Başhan, and K. Yigit, ‘Experimental energy and exergy analyses of ship refrigeration system operated by frequency inverter at varying sea water temperatures’, *Journal of the Brazilian Society of Mechanical Sciences and Engineering*, vol. 44, no. 4, p. 133, Apr. 2022, doi: 10.1007/s40430-022-03439-5.

[2] H. Kepekci, ‘A study on the performance of the various refrigerants on the two-stage vapor compression refrigeration system with a flash chamber for ships’, *International Journal of Low-Carbon Technologies*, vol. 20, pp. 690–701, Jan. 2025, doi: 10.1093/ijlct/ctaf049.

[3] J. Zhu, D. Yang, Q. Zhang, and J. Xie, ‘Performance analysis of multi-refrigerant multi-variable environment refrigeration system based on marine cold chamber’, J Phys Conf Ser, vol. 2195, no. 1, p. 012037, Feb. 2022, doi: 10.1088/1742-6596/2195/1/012037.

[4] J. Zhang, N. Mei, and H. Yuan, ‘Design, analysis, and operation optimisation of a shipborne absorption refrigeration–ice thermal storage system based on waste-heat utilization’, Thermal Science and Engineering Progress, vol. 53, p. 102720, Aug. 2024, doi: 10.1016/j.tsep.2024.102720.

[5] K. Shestopalov, O. Konstantinov, V. Ierin, and O. Khliyeva, ‘Marine Heat-driven Ejector Refrigeration Machine for Air-conditioning System with Thermal Energy Storage Unit’, Naše more, vol. 71, no. 2, pp. 84–90, Nov. 2024, doi: 10.17818/NM/2024/2.3.

[6] R. Llopis, D. Sánchez, R. Cabello, J. Catalán-Gil, and L. Nebot-Andrés, ‘Experimental analysis of R-450A and R-513A as replacements of R-134a and R-507A in a medium temperature commercial refrigeration system’, International Journal of Refrigeration, vol. 84, pp. 52–66, Dec. 2017, doi: 10.1016/j.ijrefrig.2017.08.022.

[7] A. Kumar, S.-Y. Yang, and C.-C. Wang, ‘Energy efficiency and heat transfer analysis of R-513A and other low GWP refrigerants alternative to R-134a in HVAC&R systems: A review’, International Communications in Heat and Mass Transfer, vol. 159, p. 108168, Dec. 2024, doi: 10.1016/j.icheatmasstransfer.2024.108168.

[8] R. Muliawan, A. A. A, T. Sutandi, and N. Nurrohman, ‘Cooling System Performance Comparison of Refrigerant R-134a and MC-134 on Ice Slush Machine’, FLYWHEEL : Jurnal Teknik Mesin Untirta, p. 1, May 2021, doi: 10.36055/fwl.v0i0.9237.

[9] A. Kumar, S.-Y. Yang, and C.-C. Wang, ‘Energy efficiency and heat transfer analysis of R-513A and other low GWP refrigerants alternative to R-134a in HVAC&R systems: A review’, International Communications in Heat and Mass Transfer, vol. 159, p. 108168, Dec. 2024, doi: 10.1016/j.icheatmasstransfer.2024.108168.

[10] ‘Pengaruh Variasi Massa Refrigeran Charge R-134a Pada proses Retrofit Pada Sistem Refrigerasi Dual Function Sebagai Air Handling Unit dan Water Chiller Terhadap Efisiensi Sistem’, in Proceeding Conference on Marine Engineering and its Application, Politeknik Perkapalan Negeri Surabaya, Jul. 2025. doi: 10.33863/cmea.v7i1.3092.

[11] H. Rusmaryadi and I. Badil, ‘STUDI PERBANDINGAN KINERJA FREEZER 1/5PK DENGAN R134a DAN MUSICOOL (MC-134)’, TURBULEN Jurnal Teknik Mesin, vol. 2, no. 2, p. 68, Jan. 2020, doi: 10.36767/turbulen.v2i2.560.

[12] A. Kumar, S.-Y. Yang, and C.-C. Wang, ‘Energy efficiency and heat transfer analysis of R-513A and other low GWP refrigerants alternative to R-134a in HVAC&R systems: A review’, International Communications in Heat and Mass Transfer, vol. 159, p. 108168, Dec. 2024, doi: 10.1016/j.icheatmasstransfer.2024.108168.

[13] Q. Chen and Y. Li, ‘Experimental Investigation on Intermittent Operation Characteristics of Dual-Temperature Refrigeration System Using Hydrocarbon Mixture’, Energies (Basel), vol. 15, no. 11, p. 3990, May 2022, doi: 10.3390/en15113990.

[14] Y. Zhu and Y. Yin, ‘Multi-criteria refrigerant screening and performance optimization comparison of a basic and composition-adjustable dual cooling source system’, *Appl Therm Eng*, vol. 239, p. 122154, Feb. 2024, doi: 10.1016/j.applthermaleng.2023.122154.

[15] ‘Pengaruh Variasi Massa Refrigeran Charge R-134a Pada proses Retrofit Pada Sistem Refrigerasi Dual Function Sebagai Air Handling Unit dan Water Chiller Terhadap Efisiensi Sistem’, in Proceeding Conference on Marine Engineering and its Application, Politeknik Perkapalan Negeri Surabaya, Jul. 2025. doi: 10.33863/cmea.v7i1.3092.

[16] B. Üğüdür, Ü. İşkan, and M. Direk, ‘Performance analysis of dual-evaporator ejector refrigeration system in different configurations: Experimental investigation’, International Journal of Energy Studies, vol. 8, no. 3, pp. 315–330, Sep. 2023, doi: 10.58559/ijes.1291259.

[17] I. Aulia, H. Haftirman, and E. T. Berman, ‘Viability of R-290 Refrigerant as Residential AC Retrofit: Effect of Charge Mass Variations’, International Journal of Innovation in Mechanical Engineering and Advanced Materials, vol. 7, no. 2, p. 53, Apr. 2025, doi: 10.22441/ijimeam.v7i2.30904.

[18] Q. Chen and Y. Li, ‘Experimental Investigation on Intermittent Operation Characteristics of Dual-Temperature Refrigeration System Using Hydrocarbon Mixture’, *Energies (Basel)*, vol. 15, no. 11, p. 3990, May 2022, doi: 10.3390/en15113990.

[19] N. Kumar, P. Kumar, and K. Goyal, ‘Performance Evaluation of Hydrofluorocarbon and Hydrocarbon Vapour Compression Refrigeration Systems: A Novel Experimental Approach’, Transactions of the Indian National Academy of Engineering, vol. 9, no. 2, pp. 529–538, Jun. 2024, doi: 10.1007/s41403-024-00481-8.

[20] S. O. Banjo et al., ‘Experimental analysis of the performance characteristic of an eco-friendly HC600a as a retrofitting refrigerant in a thermal system’, J Phys Conf Ser, vol. 1378, no.

4, p. 042033, Dec. 2019, doi: 10.1088/1742-6596/1378/4/042033.

[21] R. Muliawan, A. A. A, T. Sutandi, and N. Nurrohman, ‘Cooling System Performance Comparison of Refrigerant R-134a and MC-134 on Ice Slush Machine’, FLYWHEEL : Jurnal Teknik Mesin Untirta, p. 1, May 2021, doi: 10.36055/fwl.v0i0.9237.

[22] T. Aized et al., ‘Energy and Exergy Analysis of Vapor Compression Refrigeration System with Low-GWP Refrigerants’, Energies (Basel), vol. 15, no. 19, p. 7246, Oct. 2022, doi: 10.3390/en15197246.

[23] M. B. Elsheniti, H. Al-Ansary, J. Orfi, and A. El-Leathy, ‘Performance Evaluation and Cycle Time Optimization of Vapor-Compression/Adsorption Cascade Refrigeration Systems’, *Sustainability*, vol. 16, no. 9, p. 3669, Apr. 2024, doi: 10.3390/su16093669.

[24] M. Setiyo *et al.*, ‘Vapor compression refrigeration system with air and water cooled condenser: Analysis of thermodynamic behavior and energy efficiency ratio’, *Teknomekanik*, vol. 7, no. 2, pp. 112–125, Dec. 2024, doi: 10.24036/teknomekanik.v7i2.31972.

[25] W. Y. Park, N. Shah, J. Y. Choi, H. J. Kang, D. H. Kim, and A. Phadke, ‘Lost in translation: Overcoming divergent seasonal performance metrics to strengthen air conditioner energy-efficiency policies’, *Energy for Sustainable Development*, vol. 55, pp. 56–68, Apr. 2020, doi: 10.1016/j.esd.2020.01.003.

[26] I Made Rasta and I Nyoman Suamir, ‘Air Conditioning System Performance of a City Hotel Appraised for Energy Use Efficiency’, Journal *of Advanced Research in Fluid Mechanics and Thermal Sciences*, vol. 83, no. 1, pp. 118–139, Jun. 2021, doi: 10.37934/arfmts.83.1.118139.

[27] B. Omidi Kashani, ‘Increase of energy efficiency ratio of a direct evaporative cooler by dynamic behavior with energy and exergy analysis’, Proc Inst Mech Eng C J Mech Eng Sci, vol. 236, no. 7, pp. 3818–3830, Apr. 2022, doi: 10.1177/09544062211042051.

[28] M. Asim, S. Khan, A. W. Zia, F. R. Siddiqui, and M. K. H. Leung, ‘Thermal performance enhancement of novel integrated vapor compression and organic rankine cycle for electricity production: a full-condensing vs. desuperheating approach comparison in ultra-low-grade waste heat recovery’, e-Prime - Advances in Electrical Engineering, Electronics and Energy, vol. 7, p. 100493, Mar. 2024, doi: 10.1016/j.prime.2024.100493.

[29] F. Toman, P. Kracík, J. Pospíšil, and M. Špiláček, ‘Comparison of water vapour condensation in vertically oriented pipes of condensers with internal and external heat rejection’, *Energy*, vol. 208, p. 118388, Oct. 2020, doi: 10.1016/j.energy.2020.118388.

[30] M. Setiyo *et al.*, ‘Vapor compression refrigeration system with air and water cooled condenser: Analysis of thermodynamic behavior and energy efficiency ratio’, *Teknomekanik*, vol. 7, no. 2, pp. 112–125, Dec. 2024, doi: 10.24036/teknomekanik.v7i2.31972.

[31] W. T. Ho and F. W. Yu, ‘Predicting chiller system performance using ARIMA-regression models’, *Journal of Building Engineering*, vol. 33, p. 101871, Jan. 2021, doi: 10.1016/j.jobe.2020.101871.

[32] Y. Zhang, H. Li, and S. Wang, ‘Energy performance analysis of multi-chiller cooling systems for data centers concerning progressive loading throughout the lifecycle under typical climates’, *Build Simul*, vol. 17, no. 10, pp. 1693–1708, Oct. 2024, doi: 10.1007/s12273-024-1167-9.